NUMERICAL METHOD OF CALCULATE ELECTROMAGNETIC ENERGY IN THE HUMAN HEAD EXPOSED TO AN RF SOURCE

Bouali Lazhar[1], Dejennah Mohammed[2], Tahmi Redouane[3]

[1] Electrical Engineering, ENP Algiers, 32 logts lycee, Kais Khenchela;
[2-3] Electrical Engineering, ENP Algiers, 10 Av. Hassan Badi, El-Harrach BP 182, Algiers, ALGERIA.

lazhar.bouali@g.enp.edu.dz

ABSTRACT

In this paper, I study numerically the behavior of the electric field inside the human head exposed to an RF source (cellular)[1]. For this study, an electromagnetic field coupling was established between an RF source and the head. And to solve the system of equations, a finite element formulation coupled to the boundary integral formulation which is adopted, the results obtained are in the form of arrows with colors in function to the intensity of the electric field $\vec{E}$. *From where we can calculate the intensity of the electric field inside the head, which allows to calculate the SAR, and make a comparison with the SAR measured at the border of head.*

Keywords: Electromagnetic Field; Human head; Mobile Phone, Electric; magnetic

INTRODUCTION

The natural electromagnetic field has been in existence for eternity and humans have lived with it, but artificial Electromagnetics have only existed in the last centuries, however there is a question that arises: is the electromagnetic field harmful to human health [2]? The aim of our research here is to answer the question above. In this article we have chosen a part of our research which consists of a numerical study of the intensity and behavior of the electric field inside the human head. In the first case we are going to use as a RF source (the mobile phone) with frequency 1800 MHz, and we suppose that this source is glued to the head of an adult then to the head of a child, and we seek the numerical results without interface between the human head and the RF source. In the second case we put an interface in Silver and we note the numerical results found. In the third case we change the interface material with the use of glass, and we calculate each time the intensity of electric field and the correspondent SAR, and the last step is the comparison between the results.

POSITION OF THE PROBLEM ON THE PHYSICAL PLANE

One of the most important aspects is the problem of diffraction of an electromagnetic wave by an obstacle of any geometric shape. As part of our work, we want to analyze the coupling of an electromagnetic wave with a human head of spherical shape. The sphere is immersed in an RF source (Mobile telephony) [3]. The interaction of the incident wave with the human head introduces the birth of a diffracted wave and a transmitted wave. The dispersion of this electromagnetic energy in the different mediums forming our physical system, directly depends on their electromagnetic characteristics $(\sigma, \varepsilon, \mu)$, Their geometric shape, the angle of incidence and the distance d between the source and the physical system hence $d = 0$ (the source is glued to the human head) here.

ISSN: 2223-9944, e ISSN: 2223-9553
www.journals.savap.org.pk

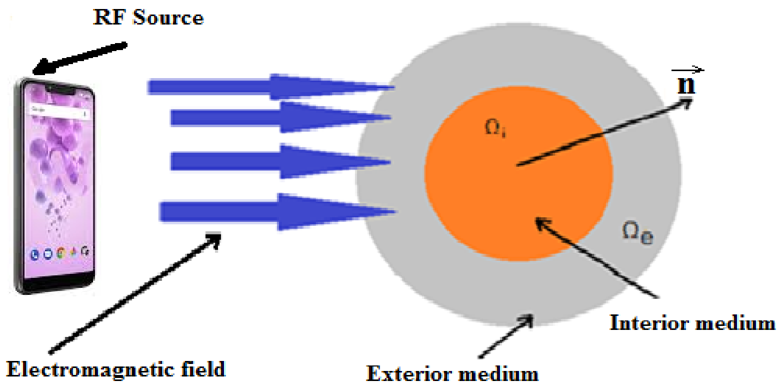

Figure 1. Physical System

The finite element method (FEM) is one of the most widely used methods for the numerical resolution of Maxwell's equations; its use is based on the transformation of partial differential equations into a system of algebraic equations. The main advantage of this method is the possibility of analyzing problems with complex geometry which may contain heterogeneous materials In general, the finite element resolution is:

i. The obtaining of the variational formulation of the problem and the definitions of the functional spaces of the admissible solutions.
ii. The realization of a mesh, corresponding to the discretization of the field of study into simple elements. In which the fields are described in terms of a finite number of degrees of free and basic functions with local support, generally polynomials. We proposed a variational formulation, in which the law of Ampere is written in the weak sense, preserving the electric field like unknown of the problem. This field is calculated in all the computation volume, where the taking into account of the external field is presented by a formulation in integral equation of the border. The use of these formulations is justified in the study of structures where the decomposition of the problem into two parts is more suited to the case treated. In the following, after having given, an integral formulation, we propose a numerical approximation of the solution by the finite element method. The use of variational methods for the resolution of electromagnetic field phenomena requires a numerical approach, posed on a space of finite dimension. For that, we adopted in a numerical model based on the discretization by finite elements in all the field of study. We have presented the mathematical framework in which these equations will be approached numerically, by giving some key properties.

Finite element spaces considered, as well as the matrices resulting from the discretization of variational formulations. This approximate solution allowed us to pass from a system of partial derivative equations to a system of algebraic equations, after the numerical resolution, which includes the calculation of elementary matrices, the corresponding physical quantity (electric field or magnetic field) is known at each point located in our finite element structure considered, as well as the matrices resulting from the discretization of variational formulations.

FORMULATION IN MAGNETIC FIELD $\vec{H}$[8]

Let $\vec{H}$ be a test vector field $\vec{H} \in (\Omega)$, , and $rot\ \vec{H} = 0$ in Ωe for $(\sigma\ = 0$.
We integrate on R^3, multiplying by the test function, which give

$$\int_{R^3} i\omega\, \mu \overrightarrow{H'}.\vec{H}\, d\Omega \; + \int_{R^3} \overrightarrow{H'} rot\, \vec{E}\; d\; \Omega = 0 \tag{1}$$

To solve the second integral, we apply some mathematical properties. Which give

$$\int_{R^3} \overrightarrow{H'} rot\vec{E} d\Omega = \int_{R^3} \vec{E} rot\vec{H} d\Omega = \int_{\Omega} \vec{E} rot\vec{H} d\Omega + \int_{\Omega e} \vec{E} d\Omega \tag{2}$$

Then (2) becomes

$$\int_{\Omega} i\omega\mu\vec{H}\overrightarrow{H'} d\Omega + \int_{\Omega} \vec{E} rot\vec{H} d\Omega + \int_{e} i\omega\mu\vec{H}\overrightarrow{H'} d\Omega = 0 \tag{3}$$

If we replace $\vec{E}$ with $(rot\frac{\vec{H}}{i\omega}\mu)$, we
obtain

$$\int_{\Omega} i\omega\mu\vec{H}.\overrightarrow{H'} d\Omega \; + \int_{\Omega} (1/i\omega\varepsilon) rot\vec{H}.\overrightarrow{H'} rot d\Omega + \int_{\Gamma} (\vec{E}\Lambda\vec{n}).\vec{H} d\Gamma = 0 \tag{4}$$

Formulation in electric field $\vec{E}$[9]

The formulation in an electric field is obtained by writing the Ampère law:

$$rot\vec{H} \;=\; \sigma\vec{E} + i\omega\, \mu\vec{E} \tag{5}$$

We make the dot product with a test function $\overrightarrow{E'}$ ($\overrightarrow{E'} \in \Omega$) and we integrate in $R3$ which gives:

$$\int_{R3} rot\; \vec{H}.\overrightarrow{E'} d\Omega \;=\; \int_{R3} (\sigma + \; i\; \omega\; \mu\; \varepsilon)\vec{E}\; \overrightarrow{E'}\; d\Omega \tag{6}$$

With:

$rot\vec{H} \;=\; 0\, in \;\; and$

$\vec{E} = 0\; in\; \Omega i.$

To solve the integral

We apply the same properties used previously so we have:

$$\int_{\Gamma} n.\left(\vec{H}\; \Lambda\; \overrightarrow{E'}\right) d\Gamma = 0$$

$$\int_{R^3} \vec{E}\;\; rot\; H\; d\Omega \; - \int_{R^3} H\; rot\overrightarrow{E'}\; d\Omega = 0 \tag{7}$$

Therefore

$$\int_{R^3} rot\vec{H}.\overrightarrow{E'} d\Omega = \int_{R^3} \vec{H} rot\overrightarrow{E'} \;\; = \int_{\Omega i} rot\overrightarrow{E'}.\vec{H}\; d\Omega + \int_{\Omega e} rot\overrightarrow{E'}.\vec{H}\; d\Omega \tag{8}$$

ISSN: 2223-9944, e ISSN: 2223-9553
www.journals.savap.org.pk

Multiply by $(-i\omega\mu)$,the formulation in $\vec{E}$ is writen :

$$-\int_{\Omega i} (\sigma\, i\omega\mu\varepsilon)\vec{E}\overrightarrow{E`}d\Omega \int_{\Omega e} \left(\frac{1}{i\omega\mu}\right) rot\vec{E}rot\acute{E}d\Omega + \int_{\Gamma} \overrightarrow{E`}(n\Lambda\, H)\overrightarrow{E`}d\Gamma = 0 \tag{9}$$

$$\int_{\Omega i} rot\vec{E}rot\vec{E}.E`d\Omega + \int_{\Omega e} (i\omega\mu\sigma - \omega^2\mu\varepsilon)\vec{E}.\overrightarrow{E`}d\Omega + \int_{\Gamma} \overrightarrow{E`}\left(n\Lambda rot\vec{E}\right)d\Gamma = 0 \tag{10}$$

Expression of the electric field in exterior medium

We have:

$$\Delta\, \vec{E}\, e\, +\, k^2\, \vec{E}e = \frac{1}{-i\omega\varepsilon_e\left(k^2 + \overrightarrow{grad}\; div\right)J_s} \tag{11}$$

$with\;\; k^2 = \omega^2\mu_e\varepsilon_e$

According to equation (11), we have

$$S(x) = -\frac{1}{\omega\mathcal{E}_e\left(k^2 + \overrightarrow{grad}div\right)J(x)} \tag{12}$$

The application of Green's function in equation (11) allows us to write:

$$\vec{E}e(x) = \int_{\Omega e} G(x,y)S\,(y)dy \tag{13}$$

Finally, we will reach our objective, where the global variational formulation of the problem is defined in all the space R^3, which gives :

$A(\overrightarrow{E_r}\,,\overrightarrow{E'})\; +\; R\;(\overrightarrow{E_r},\overrightarrow{E'})\;\; = S(\overrightarrow{E_s}\,,\overrightarrow{E'})$

$$R\left(\overrightarrow{E_r},\overrightarrow{E'}\right) = -i\omega\mu_e\left(\int_{\Gamma} \frac{k(x)}{2}\overrightarrow{E'}(x)d\Gamma_x + \int_{\Gamma} T\vec{K}(x).\overrightarrow{E'}(x)d\Gamma_x\right) \tag{14}$$

VARIATIONAL DISCRETIZATION OF THE PROBLEM

We recall the variational formulation:

$$A(\overrightarrow{E_r}\,,\overrightarrow{E'})\; +\; R\;(\overrightarrow{E_r},\overrightarrow{E'})\;\; = S(\overrightarrow{E_s}\,,\overrightarrow{E'})$$

Given that the formulation of the problem is obtained previously, we will thus proceed to the next stage, which consists in the realization of the mesh, by decomposing the variational problem, presented above into elements of edges in an approximate space.

Discretization of the form a $(\mathbf{E_r}, \mathbf{E}')$[11]

Then, for each tetrahedron element, the approximate electric field is written:

$$\overrightarrow{E'}\; = \sum_{i=1}^{6} \overrightarrow{Ei}\, Wi \tag{15}$$

The electric field $\overrightarrow{Ei}$ is a scalar quantity, it represents the degree of freedom per edge i.By taking this interpolation into account, the approximate test field $\overrightarrow{E'}$ is therefore written:

$$E' = \sum_{i=1}^{6} Ei\, Wi$$

We have:

$$a(E_r, E_s) = \int_{\Omega} rot\, E_r . RotE'\, d\Omega + \int_{\Omega} (i\omega\mu\sigma - \omega^2\mu\varepsilon) E_r E' d\Omega \tag{16}$$

The approximate form is obtained by decomposing $a\,(E_r\,, E')$ into an edge element, which gives:

$$a(\,E_r, E') = \sum_{tet}^{6}\sum_{i=1}^{6} E_i \int_{\Omega} rotW_i rotW_j d\Omega + (i\omega\mu\sigma - \omega^2\mu\varepsilon)\sum_{tet}^{6}\sum_{i=1}^{6} E_i \int_{\Omega} W_i W_j d\Omega \tag{17}$$

The form given by (4) can be written in the following matrix form:

$$a\,(\,E_r, E') = E\{[T1] + (i\omega\mu\sigma - \omega^2\mu\varepsilon)[T2\,]\} \tag{18}$$

Where $\vec{E}$ is the unknown vector.

$$\vec{E} = [E_1\,, E_2, \ldots .\, E_N\,]^T$$

With T1 and T2 are time-independent matrices whose elementary terms are given by:

$$[\,T1]_{ij} = \int_{\Omega} rotW_i rotW_j d\Omega\; = 4\int_{\Omega} (\nabla\lambda_{ai}\lambda_{bi})\big(\nabla\lambda_{bi}\lambda_{bj}\big) d\Omega \tag{19}$$

$$[T2]ij\;\; = \int_{\Omega} W_i W_j d\Omega = \int_{\Omega} (\lambda_{ai}\nabla\lambda_{bi} - \lambda_{bi}\nabla\lambda_{ai}).\big(\lambda_{aj}\nabla\lambda_{bj} - \lambda_{bj}\nabla\lambda_{aj}\big) \tag{20}$$

Construction and calculation of the second member (S)

The term linked to the source is given by

$$S\,\big(\overrightarrow{E_s}, \overrightarrow{E'}\big) = -\int_{\Omega} rot\overrightarrow{E_s} rot\overrightarrow{E'} d\Omega - \int_{\Omega} (i\omega\mu\sigma - \omega^2\mu\varepsilon)\overrightarrow{E_s} - \int_{\Gamma} \overrightarrow{E'}\vec{n}\Lambda rot\overrightarrow{E_s}) d\Gamma$$

The approximate form of S is written:

$$S\big(\overrightarrow{E_s}, \overrightarrow{E'}\big) = \sum_{tet}^{6}\sum_{i=1}^{6} E_{si} \int_{\Omega} rotW_i rotW_j d\Omega$$
$$- (i\omega\mu\sigma - \omega^2\mu\varepsilon)\sum_{tet}^{6}\sum_{i=1}^{6} E_{si}\int_{\Omega} W_i W_j d\Omega + \sum_{tet}^{3}\sum_{i=1}^{3} E_{si}\int_{\Gamma} (n\Lambda rotW_i) W_j d\Gamma \tag{21}$$

The elementary matrices are defined by

$$[S_1]_{ij} = \int_{\Omega} rotW_i rotW_j d\Omega = 4\int_{\Omega} (\nabla\lambda_{ai}\nabla\lambda_{bi})(\,\lambda_{aj}\nabla\lambda_{bj})\, d\Omega$$

$$[S_2\,]ij\;\; = \int_{\Omega} W_i W_j d\Omega = \int_{\Omega} (\lambda_{ai}\nabla\lambda_{bi} - \lambda_{bi}\nabla\lambda_{ai})\,(\lambda_{aj}\nabla\lambda_{bj} - \lambda_{bj}\nabla\lambda_{aj})\, d\Omega$$

ISSN: 2223-9944, e ISSN: 2223-9553
www.journals.savap.org.pk

$$[F]_{ij} = \int_{\Gamma} (n\,\Lambda rotW_i)W_j d\Gamma = 2\int_{\Gamma} [n\,\Lambda(\nabla\lambda_{ai}\nabla\lambda_{bi})](\lambda_{aj}\nabla\lambda_{bj} - \lambda_{bj}\nabla\lambda_{aj})d\Gamma \quad (22)$$

So the second member S is given as follows

$$S(E_s, E') = E_s\{[S_1] - (i\omega\mu\sigma - \omega^2\mu\varepsilon)\,[S_2] + [F]\,\}$$

Breakdown of the edge term [24]

The calculation of the edge term is established in (14)

$$R(\overrightarrow{E_r}, \overrightarrow{E'}) = -i\omega\mu_e(\int_{\Gamma} \frac{k(x)}{2}\overrightarrow{E'}(x)d\Gamma_x + \int_{\Gamma} T\vec{K}(x)\overrightarrow{E'}(x)d\Gamma_x) \quad (23)$$

Or

$$T\,\vec{K}(x) = \vec{n} \wedge \int_{\Gamma} \overrightarrow{grad}yG(x,y) \wedge \vec{K}(y)d\Gamma_y$$

The discretization of $R(\vec{E}_r\,, \vec{E}')$,, involves a test field, such as:

$$\vec{E}'(x) = W_j(x)Wj(x) \quad (24)$$

Using the fictitious current relation K the term $T\,\vec{K}(x)$ is approached as

$$[T\,K(x)E'(x)] = \sum_{j}^{Na}\sum_{i}^{Ne}\{\iint_{\Gamma\Gamma} \frac{[n\,\Lambda((x-y)\Lambda W_i(y)]W_j(x)}{|x-y|^3}d\Gamma_x d\Gamma_y\} \quad (25)$$

$$(Q_i^{-1}B)_{ij}\,E_j$$

The system of equations given above can be written in the following matrix form

$$(M)_{ji} = \iint_{\Gamma\Gamma} \frac{\{n\,\Lambda[(x-y)\Lambda W_i(y)]\}W_j(x)}{|x-y|^3}d\Gamma_x d\Gamma_y \quad (26)$$

So, the relation (25) is written:

$$[TK(x)\,, E'(x)] = \sum_{j}^{Na}\left\{\sum_{i}^{Ne}(M)_{ji}(Q_i^{-1}B)_{ij}\right\}E_j \quad (27)$$

We have directly defined the first term of $R\;(Er\,, E''{}')$

$$\frac{1}{2}[TK(x), E'(x)] = \frac{1}{2}\sum_{i}^{Ne} P_i \int_{\Gamma} W_j(x)W_i(x)d\Gamma_x \quad (28)$$

From where

$$\frac{1}{2}[TK(x), E'(x)] = \frac{1}{2}\sum_{j}^{Na}\left\{\sum_{i}^{Ne}\left(B^{t}\right)_{ji} ji(Q_i^{-1}B)_{ij}\right\} \quad (29)$$

B^{t} is the transpose of the matrix B

Finally, the global matrix of the edge term, noted R_m in edge variables, is written as

$$R_m = \sum_{i}[\frac{1}{2}B^{t} + M]_{ji}(Q_i^{-1}B)_{ij}$$

Or

$$R_m = [\frac{1}{2}B^{t} + M]Q_i^{-1}B$$

Taking into account these elementary matrices (27), (28) and (29), the global matrix system, denoted MAT, is therefore written:

$$MAT = E\{[T_1] + (i\omega\mu\sigma - \omega^2\mu\varepsilon)[T_2] + R_m\} = S$$

After the imposition of the appropriate boundary conditions, the results are obtained by solving for a given excitation frequency, a matrix equation of the type$[A]\ x = b$, where$[A]$ is a hollow matrix with complex coefficients.

NUMERICAL IMPLENTATION

Our model's simulation is presented in the form of a human head and an interface which presents two mediums. The exterior is an interface and the interior is the human brain of an adult and a child. We have considered the two homogeneous, isotropic, and dispersive mediums. We have chosen frequencies of the electromagnetic source, f = 1800MHz, for 4G standard

Electrical characteristics of the two mediums for (f = 1800 MHz)[25]

Concerning the ELM source, this is characterized by

-frequency; f = 1800MHz;
-Current:$Js = 200\ A/m^2$.
<u>Brain characteristics (interior medium)</u>
-Electrical permittivity: $\varepsilon_{riC} = 43{,}22$
-Electrical conductivity: $\sigma_{iC} = 1{,}29\ S/m$.
-Permeability: $\mu = 1$
<u>Electrical characteristics of the silver interface</u>
- Electrical conductivity $\sigma_{e1} = 6{,}25\ 10^7\ \frac{S}{m}$
-Electrical permittivity: $\varepsilon_{re1} = 2{,}5$.
-Permeability : $\mu = 1$

The meshing of the domain of study

The structure mesh was obtained with the meshing tool CELLULAIR 003 characterized by a tetrahedral discretization data on the mesh realize. Our meshing tool allowed us to read the mesh, as follows:

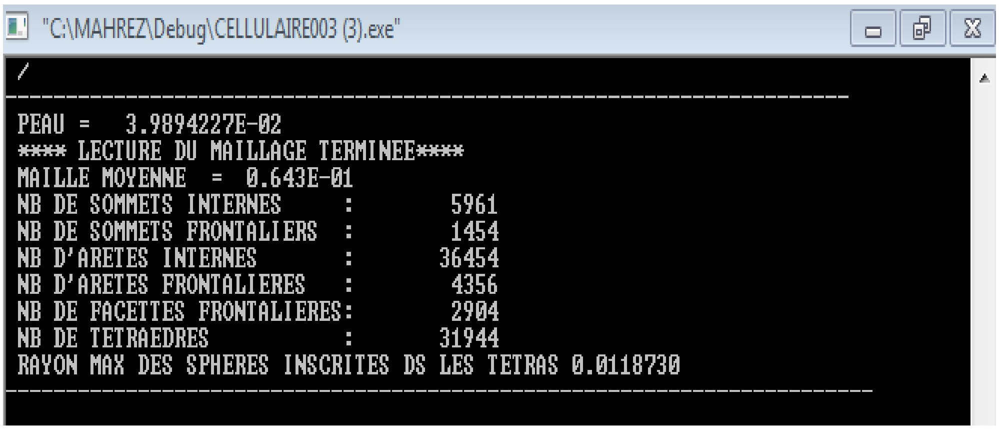

(a)

ISSN: 2223-9944, e ISSN: 2223-9553

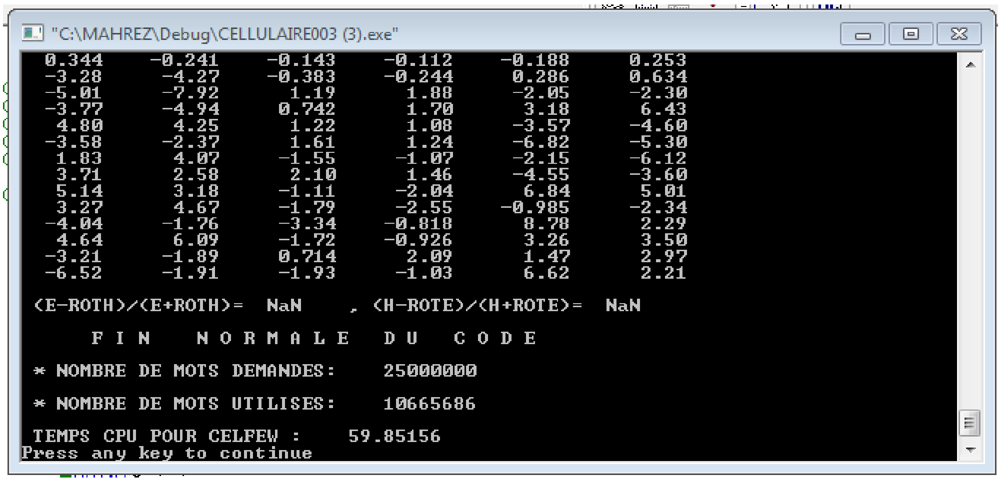

```
"C:\MAHREZ\Debug\CELLULAIRE003 (3).exe"
 0.344    -0.241    -0.143    -0.112    -0.188     0.253
-3.28     -4.27     -0.383    -0.244     0.286     0.634
-5.01     -7.92      1.19      1.88     -2.05     -2.30
-3.77     -4.94      0.742     1.70      3.18      6.43
 4.80      4.25      1.22      1.08     -3.57     -4.60
-3.58     -2.37      1.61      1.24     -6.82     -5.30
 1.83      4.07     -1.55     -1.07     -2.15     -6.12
 3.71      2.58      2.10      1.46     -4.55     -3.60
 5.14      3.18     -1.11     -2.04      6.84      5.01
 3.27      4.67     -1.79     -2.55     -0.985    -2.34
-4.04     -1.76     -3.34     -0.818     8.78      2.29
 4.64      6.09     -1.72     -0.926     3.26      3.50
-3.21     -1.89      0.714     2.09      1.47      2.97
-6.52     -1.91     -1.93     -1.03      6.62      2.21

 <E-ROTH>/<E+ROTH>=  NaN    , <H-ROTE>/<H+ROTE>=  NaN

     F I N    N O R M A L E    D U    C O D E

 * NOMBRE DE MOTS DEMANDES:     25000000

 * NOMBRE DE MOTS UTILISES:     10665686

 TEMPS CPU POUR CELFEW :    59.85156
Press any key to continue
```

(b)

Figure 2. (a), (b): Reading of mesh of our model

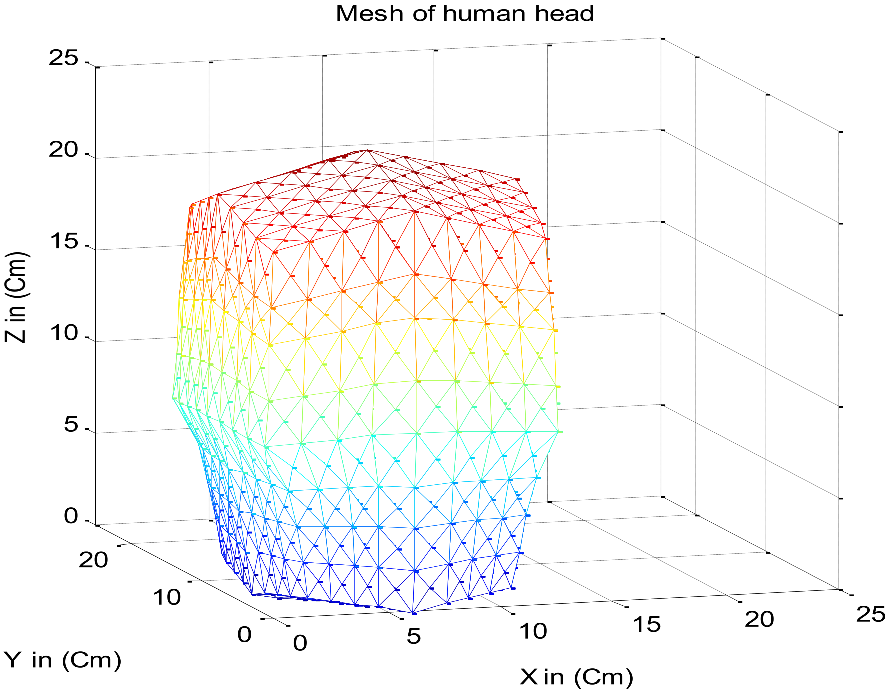

Figure 3. Mesh of our model (human head)

Numerical results obtained from an RF source glued to the human head

We performed numerical tests, using our calculation code that we developed:

-The first test: the electromagnetic source glued to the human head, and we had a frequency

f = 1800 MHz, with the variation of the electrical characteristics of the exterior medium of our model which is obtained from the setting up of our interface by different materials or we used for this test, Silver($\mu_{e1}, \varepsilon_{e1}, \sigma_{e1}$),

After each test we obtained numerical results in the form of a cartography, which represents the behavior and the intensity with the colors of the electric field inside the human head.

Numerical results without interface

The source, it is characterized by: frequency

$f = 1800MHz$, current $Js = 200\ A / m2$, the distance between the source and the human head $d = 0.005\ m$ (the source glued to the human head)

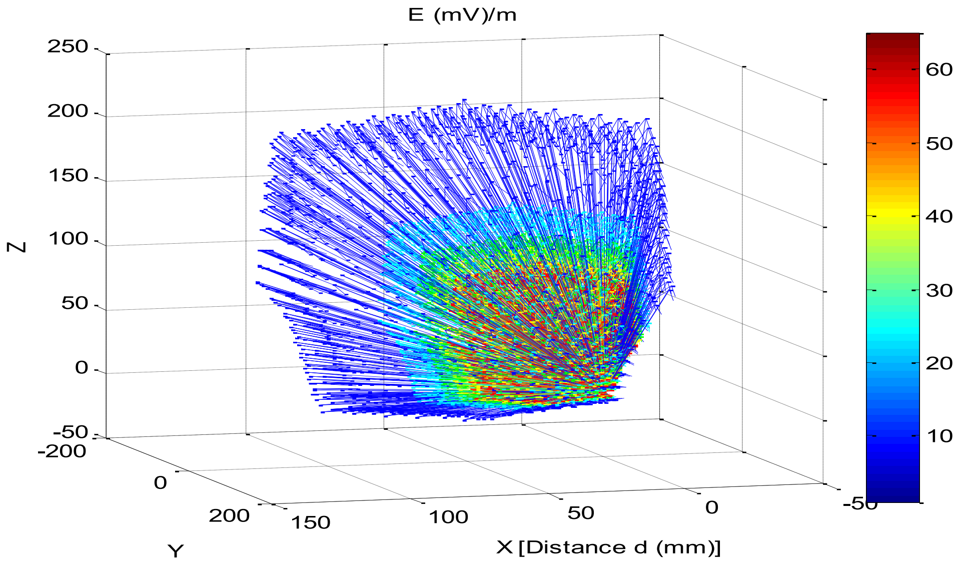

Figure 4. Electric field intensity $\vec{E}$ (mV / m), Human Head without interface

The results with a Silver interface

The source, it is characterized by: $f = 1800MHz$ current $Js = 200\ A / m2$, the distance between the source and the human head $d = 0.005\ m$ (the source glued to the head)

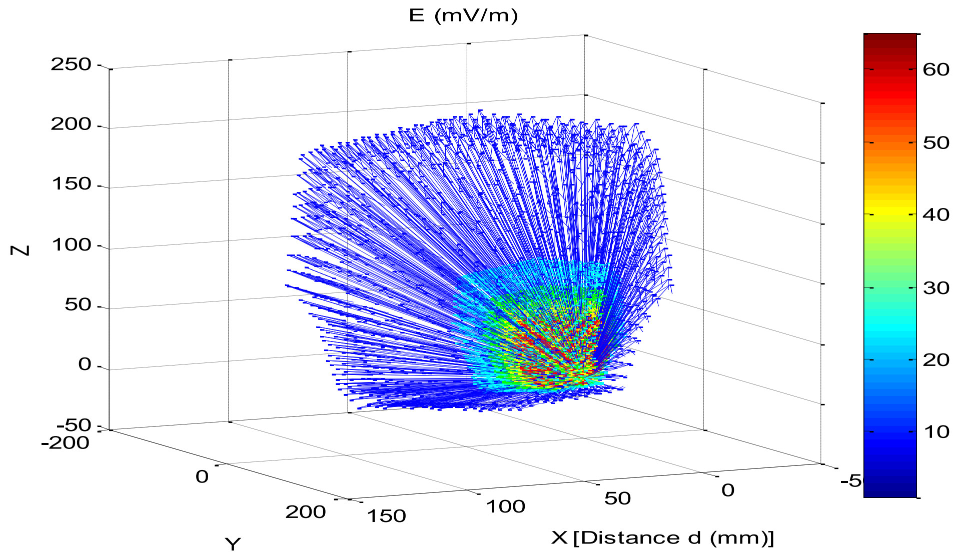

Figure 5. Electric field intensity $\vec{E}$ (mV/ m) Human Head with Silver interface

FORMULATION AND CALCLATE OF SAR

The formulation of specific absorption rate [28]:

$$SAR = \frac{\sigma E^2}{m_d} \tag{30}$$

$$Incident\ power\ density = \frac{E^2}{377}$$

Where, σ = Conductivity of Material, E = Electric Field,
m_d = Mass Density

$$The\ SAR\ measured\ (SAR) = 6.78\ W/kg\ [29]$$

From the numerical results presented in figures (4) and (5) we calculated the SAR, without interface and with silver interface, where is shown in the following table.

Table 1. The SAR inside human head, without interface and with Silver interface

Distance (mm)	SAR (W/kg)without interface	SAR (W/kg) with silver interface
10	6.78	6.78
20	8.43	6.93
30	9.56	5.56
40	8.12	3.12
50	7.12	2.12
60	2.32	1.32
70	1.45	0.45
80	0.56	0.36
90	0.39	0.34
100	0.34	0.30
110	0.28	0.28

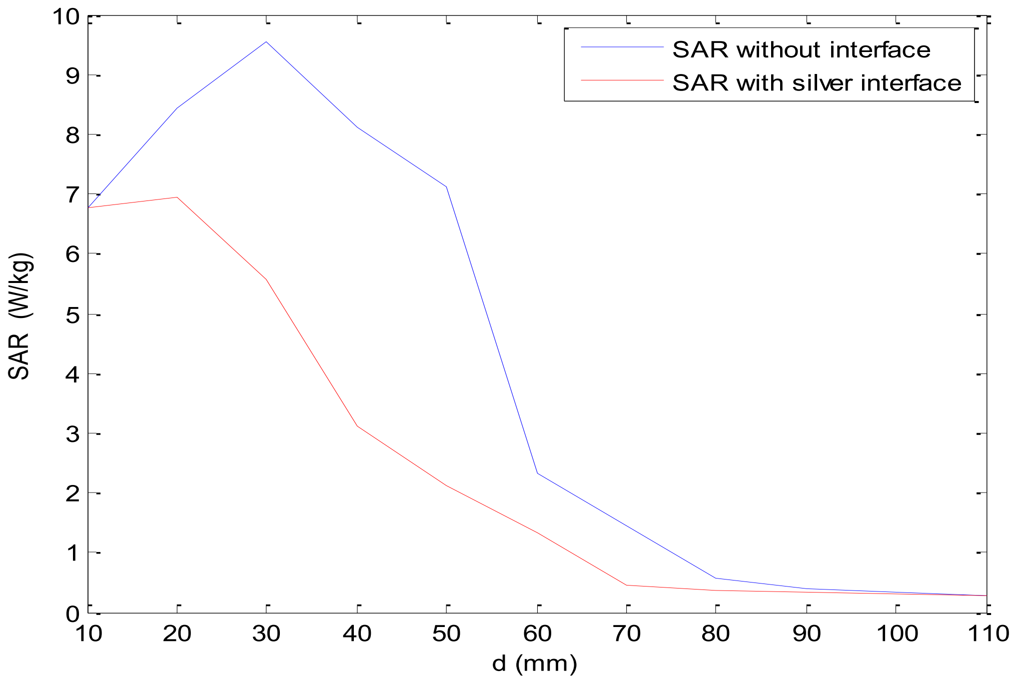

Figure 6. The SAR inside human head, with a silver interface and without interface

INTERPRETATION AND DISCUSSION

Using our numerical method, we can calculate the electric field $\vec{E}$ at each point inside the human head, which is practically non- measurable. We have also noticed that for an electromagnetic source glued to the human head, and of frequency, (f = 1800), the electric field $\vec{E}$ varies according to the distance d inside the human head, which implies the variation of the DAS [equation (30)], For our tests, with a model without interface and another with an interface in Silver, we have the numerical results indicated in figures (4) and (5) from which we withdraw the values of the electric field $\vec{E}$ inside the human head, which makes it possible to calculate the SAR inside it, hence the SAR values are shown in TableI1. And shown graphically in Fig. 6. For a model with interfaces and without interface. We noticed

ISSN: 2223-9944, e ISSN: 2223-9553
www.journals.savap.org.pk

that the SAR had an increase or a peak just after the entry of the electric field inside the human head Fig. 5. After the SAR decreased in function of the distance (d) in the human head, and for a Silver interface we notice the disappearance of the peak.

For giving to the explanation of this peak we use equation (30), hence the SAR and as a function of σ (the electrical conductivity of the medium) [26].

And therefore the exterior medium is the air which conductivity σ which is very small compared to the interior medium, which is the brain. Which explains the increase in the value of the SAR, and also explains the elimination of the peak if the interface and in Silver, hence the value of the electrical conductivity σ, and greater than that of the interior medium which a brain.

We therefore observed that the SAR measured on the outside and smaller than that on the inside just after the entry of the electric field. And for the correction we used interface in Mittal of silver to have the same SAR measured at the exterior [29] of the human head and that interior (brain).

CONCLUSION

This part of our work is a subject of a contribution to search for the problems of the interaction of the electromagnetic fields with the human head, we have defined the physical system and posed the problem, from Maxwell's equations in a harmonic regime, a synthesis of various variational formulations was done to solve the problem numerically. For the implementation of the proposed formulations, we used the finite element method. By adopting digital finite element resolution coupled with the integral boundary method, we finally had a digital result in the form of a map containing the colored arrows that represented the electric field and its intensity inside the human head. The results obtained for a frequency f = 1800 MHz and a source stuck to the head. We used the behavior of the electric field to calculate its intensity and the SAR for certain points inside the human head. Finally, we compared the results obtained for the SAR calculated inside the human head and the SAR measured at the limit. And we found that the SAR inside underwent an increase just at the entry of the electric field at the Inside the human head, this increase which is in the form of a peak and for the correction we have proposed a Silver interface which gave us good results.

REFERENCES

IEEE. 'Standard for safety levels with respect to human exposure to radio frequency electromagnetic fields, 3 kHz to 300 GHz'. Document IEEE C95-1/2005. New York: Institute of Electrical and Electronics Engineers, 19 Avril 2006.

NRPB. 'Board statement on restrictions on human exposure to static and time varying electromagnetic fields end radiation'. Documents of the NRPB, vol. 4, No. 5. Chilton, Didcot, U.K.: National Radiological Protection Board, 1993.

CENELEC. 'Human exposure to electromagnetic fields'. European Prestandard 50166-1 and50166-2. Brussels, 1995. WHO/IRPA,1993),fields (up to 300 GHz)'. Health Phys. 74:494-522, 1998.

Recommendation 1999/519/CE. 'La Recommandation du Conseil du 12 juillet 1999 relative à la limitation de l'exposition du public aux champs électromagnétiques (0 Hz à 300 GHz).' Juillet 1999.

Italy. 'Regulation for the determination of ceiling values of radiofrequencies compatible withhuman health'. Decree 10, Sep. 1998, No. 381. Gazzetta Ufficiale dellaRepubblica Italiana n. 257 del3-11-1998 (In Italian).

Aubineau P., Bardou A., Dixsaut G., Goldberg M. De Seze R., Veyret B., Zmirou D.(2001). 'Lestéléphones mobiles, leurs stations de base et la santé. Etat des connaissances et recommandations'.Rapport au Directeur Général de la Santé, Janvier 2001.

M.Djennah, (2006). Théorie des champs électromagnétiques »,Polycopie , cours de 1er année Magister, EMP, 2005- 2006.

M. Djennah, B. Bandelier, (1997). Computation of Electric Charges and Eddy Currents with an E- Formulation », IEEE Trans. *on Magnetics, 33*(2), march 1997.

Joubert V., (2006). Thèse de biologie, sciences, sante de l'université de Limoges : 'Exposition in vitro de cellules neuronales aux radiofréquences :étude de l'apoptose.

A. Bossavit, (2005). Electromagnétisme, en vue de la modélisation», Edition Springer VerlagFrance , Paris, 1993. 2005.

F. Tahar Belkacem, (2005). Modélisation numérique du champ électromagnétique HF à la surface d'une couche ferromagnétique et conductrice» Thèse Magistère. EMP .

De Seze R. (1999). 'Radiotéléphones cellulaires et sante : mise au point des recherches portant sur la sante chez l'homme', Radioprotection Vol. 34, n° 4, pages 479 a 490.

Wong M. F., Wiart J.(2005). 'Modeling of electromagnetic wave interactions with the human body', *Competes Rend us Physique, 6(* 6), pp. 585-594, July-August 2005.

Laval L. (nd). Thèse d'électronique de l'université de Limoges Cnception et caractérisation dosimétrique de dispositifs micro-ondes pour des applications bio électromagnétiques, liée à l'utilisation des téléphones portables', n°: 29-99.

Luc J., (2002). Thèse d'électronique de l'université de Limoges Interaction des ondes électromagnétiques avec le vivant. Etude et dosimétrie numérique de systèmes d'exposition aux fréquences micro-ondes, n° d'ordre : 41.

Collin A.,(2007). Thèse d'électronique de l'université de Limoges :'Dosimétrie de systèmes d'exposition pour l'étude in vivo ou in vitro des interactions des ondes électromagnétiques décimétriques et centimétriques avec le vivant', n° d'ordre : 22.

Kuster N., Schonborn F.(2000). 'Recommended minimal requirements, development guidelines for exposure setups of bio-experiments addressing the health risk concern of wireless communications', Bio electromagnetics,Vol. 21, Issue 7, pp. 508-514, October 2000.

Dhahi S.J., Habash W.Y., and Al-Hafid H.T. (1982). 'Lack of mutagenic effects on conidia of asper Gillusamste lodami irradiated by 8.7175-GHz CW microwaves.' J. Microwave Power, 1982, vol. 17, p. 345-351.

Z.Ren, F. Bouillault, « A new Hybrid model using Electric Field Formulation for 3D Eddy current Problems », IEEE Trans. On Magnetics, vol. 26, n°2, march 1999.

M. Remaki, « Méthodes numériques pour les équations de Maxwell instationnaires en milieu hétérogène », Thèse de Doctorat de l'Ecole Nationale des Ponts et Chaussées, décembre1999.

G.Orjubin, (2005). *Modélisation modale d'une chambre réverbérante par méthode des éléments finis.* Thèse de Doctorat de l'Université Marne- la Vallée, mai 2005.

L.Pichon, (1996). *Comparison between tangentially continous vector finite elements for eigen value problems in 3D cavities* . IEEE Trans. On Magnetics, vol.32, n°3, may1996.

O.Ouchetto (2006). Modélisation Large Bande de Metamateriaux Bianisotropes et de surfaces structurées ; Thèse de Doctorat de l'Université Paris-Sud XI, décembre 2006.

S. Gabriel, RW Lau et C. Gabriel, (1996). The dielectric properties of biological tissues : III. Parametric models for the dielectric spectrum of tissues. *Phys. Med. Biol, 41*(11) :2271–2293, 1996.

Gabriel, C.(1996). *"Compilation of the dielectric properties of body tissues at RF and microwave frequencies,"* Armstrong Lab., Brooks Air Force Base, TX, Brooks Air Force Base Tech.Rep. AL/OE-TR-1996-0037, June 1996.

S. Khoudiri, (2006). Etude du Comportement d'une Enceinte Métallique sous l'Effet d'un Rayonnement Electromagnétique Application à la CEM » Thèse Magistère. EMP. 2006.

WHO (2011). Research Agenda for Radio Frequency Fields, World Health Organization. (2011). Available from:http://edition.cnn.com/2011/HEALTH/05/31/who.cel.phones/index.html

Yu, Q.and O.P.Gandhi, (1999). "An automated SAR measurement system for compliance testing of personal wireless devices," IEEE Trans. EMC, Vol.41, No.3, 234–244, 1999.

ISSN: 2223-9944, e ISSN: 2223-9553